Journal of Manufacturing Processes 32 (2018) 213–221

Contents lists available at ScienceDirect

Journal of Manufacturing Processes

journal homepage: www.elsevier.com/locate/manpro

Reducing edge chipping defect in rotary ultrasonic machining of optical glass by compound step-taper tool

Jianjian Wang [a,b], Pingfa Feng [a,c], Jianfu Zhang [a,*]

[a] State Key Laboratory of Tribology, Tsinghua University, Beijing, China
[b] Department of Mechanical and Automation Engineering, The Chinese University of Hong Kong, Hong Kong, China
[c] Division of Advanced Manufacturing, Graduate School at Shenzhen, Tsinghua University, Shenzhen, China

ARTICLE INFO

Article history:
Received 1 June 2017
Received in revised form 24 January 2018
Accepted 2 February 2018
Available online 20 March 2018

Keywords:
Rotary ultrasonic machining
Edge chipping
Brittle material
Optical glass
Tool design

ABSTRACT

The machining induced edge chipping of hole manufacturing restricts the productivity and design capability of products made from brittle materials. Rotary ultrasonic machining (RUM) has been sufficiently proved as a suitable approach for hole drilling in brittle materials with reduced cutting force and improved hole edge quality. However, apparent edge chipping is still an important restriction of RUM application. In this study, a compound step-taper tool for RUM was designed to further reduce the edge chipping defects via tool design. RUM tests on quartz glass were conducted to evaluate the effectiveness of the compound step-taper tool. The experimental results demonstrated that the compound tool could reduce the edge chipping size at the hole exit and entrance by 60%–80% and 35%–50%, respectively. The mechanism of edge chipping reduction at the hole exit is that cutting force decreased as the undrilled thickness decreased. This is due to the wedge-type contact structure between the tool's taper face and the workpiece material. Furthermore, the edge chipping reduction at the hole entrance occurs because of the shielding effect of residual cracks. Residual cracks produced by the second outermost abrasives of the tool's taper face suppressed the initiation and propagation of lateral cracks that were produced by the outermost abrasives of the tool's taper face. Theoretical analysis indicated that the compound tool step is beneficial for guaranteeing the effectiveness of tool's taper face.

1. Introduction

Brittle materials such as optical glasses and advanced ceramics are difficult to machine using a conventional metal cutting method [1]. Brittle materials usually have high hardness that results in severe tool wear, which suppresses the improvement of machining efficiency [2]. Meanwhile, low toughness can induce undesirable defects, reducing the rate of finished products [3]. The machining efficiency and quality improvement of brittle materials are still challenging and critical for corresponding application extensions [4]. Various conventional and unconventional methods have been introduced for machining brittle materials, such as conventional diamond grinding [5], ultrasonic machining (USM) [6], ultrasonic vibration assisted grinding [2,7–9], laser machining [10–12], electrical discharge machining [13], and rotary ultrasonic machining (RUM) [14–16].

Through-hole manufacturing is commonly required in products made from brittle materials. An improvement in the hole exit quality is quite desired because the severe edge chipping defect at the hole exit severely affects productivity as well as design capability [17]. RUM has been sufficiently proved as a suitable method for hole drilling in brittle materials with reduced cutting force and improved hole exit quality [18–21]. As illustrated in Fig. 1, a rotating electroplated diamond tool can vibrate ultrasonically with low amplitude while it moves in the feed direction toward the workpiece during RUM. Moreover, an apparent edge chipping defect at hole exits during RUM remains inevitable [22].

Many investigations have been conducted to reduce edge chipping in RUM. Wang et al. considered the edge chipping formation at the hole exit as the propagation of machine induced subsurface cracks under the cutting force (thrust force) [23]. Then, the relationship between the edge chipping size and the trust force was modeled mechanistically on the basis of the proposed formation mechanism of edge chipping [18]. It was discovered that the thrust force was the main parameter that affects the edge chipping size. Moreover, a higher spindle speed or lower feed rate results in a lower edge chipping size, and this is accompanied by a weaker cut-

* Corresponding author at: Department of Mechanical Engineering, Tsinghua University, 100084, Beijing, China.
E-mail address: zhjf@mail.tsinghua.edu.cn (J. Zhang).

https://doi.org/10.1016/j.jmapro.2018.02.001
1526-6125/

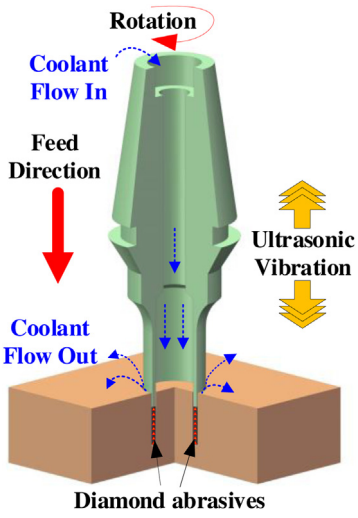

Fig. 1. Illustration of RUM.

ting force [18]. Also, Cong et al.'s work on silicon ceramics [24] and Jiao et al.'s work on alumina ceramics [25] indicated a similar relationship between the edge chipping size and the thrust force as the results documented in Wang et al.'s work. Liu et al. used the desirability functions and response surface analysis to minimize the edge-chipping size during RUM of ceramic materials [26]. In addition to optimizing the processing parameters, Gong et al. proposed an effective method to reduce the edge chipping size, which was additional support at the hole exit [27]. Moreover, Li et al. and Chen et al. also proposed that an increase in the support length contributed to improvement in the hole exit quality [22,28]. However, the support addition increased the manufacturing complexity, but cannot be used in many drilling situations.

The tool design constitutes another low cost approach for the edge chipping size reduction of the machined holes [17]. According to the positive dependency of the edge chipping size on the thrust force, the wall thickness decrease of the diamond core tool proved effective in further reducing the edge chipping size. This occurred because of reduced thrust force. However, decreasing the tool wall thickness would increase the tool manufacturing complexity because of the weaker rigidity of the thinner-wall tool, and also restrict the increase in drilling efficiency because of the strength limitation of the tool with a thinner-wall. Tool shape optimization is another method for reducing the edge chipping size. Two types of specially shaped tools have been reported to have superior potential for reducing edge chipping, and these are the step-type tool and the taper-type tool. Wang et al. used the step-type diamond core tool for RUM of sapphire and quartz glasses, and the experimental results demonstrated that the well-designed step-type tool reduced the edge chipping size by up to 50% [29]. From the experimental and finite elements modeling (FEM) results, Qin et al. reported that the taper-type tool was effective for improving the hole exit quality [30]. Wang et al. experimentally investigated the effect of the taper angle on the taper-type tool effectiveness in terms of reducing edge chipping [31].

In this study, the good performances of both the step-type tool and taper-type tool were taken advantage of by using a compound step-taper tool to reduce the edge chipping size at the hole exit during RUM of brittle materials. Drilling tests on quartz glass were conducted to evaluate the feasibility of the compound drill on reducing edge chipping. The cutting force variation at the hole exit was used to observe the reduction mechanism of edge chipping via the compound drill. A theoretical method was used for role analysis of the step face in the effectiveness of the compound tool.

2. Fundamentals of edge chipping reduction via tool design

When a common tool is used, the method of optimizing parameters cannot improve the hole exit quality completely, often at the sacrifice of machining efficiency. As presented in Fig. 2(a), when a common tool is used to drill holes in brittle materials, the undrilled thickness (d) decreases gradually as the drilling depth increases. The cutting force varies slightly. As illustrated in Fig. 2(b), when the undrilled thickness decreases to a certain value (d_t), edge chipping forms; d_t is also called the edge chipping thickness. According to the authors' previous experimental results, d_t is directly proportional to the edge chipping width (d_s) [23]. Moreover, d_t and the

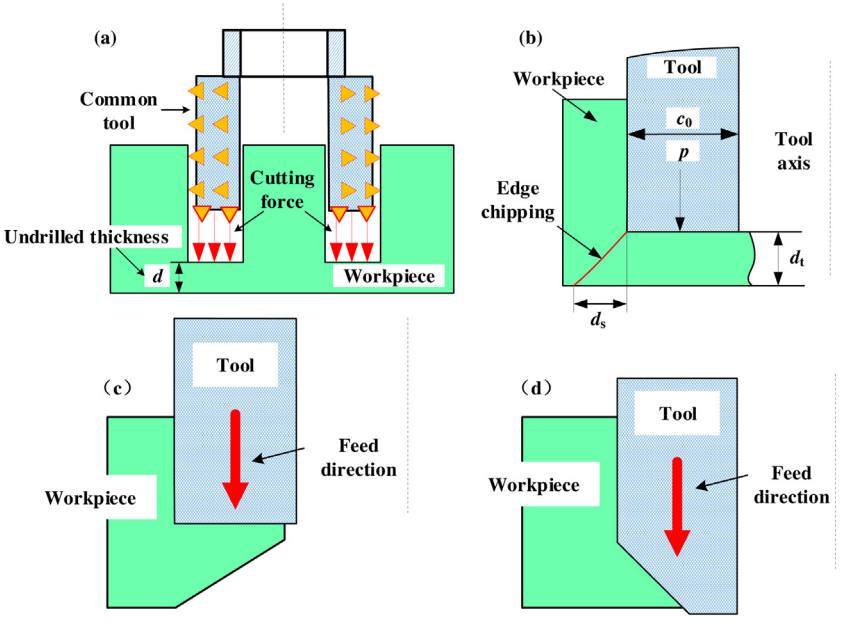

Fig. 2. Edge chipping formation. (a) Illustration of undrilled thickness using a common diamond core tool. (b) Relationship between edge chipping thickness and cutting force. (c) and (d) Two types of wedge-type contact structures between the tool and workpiece.

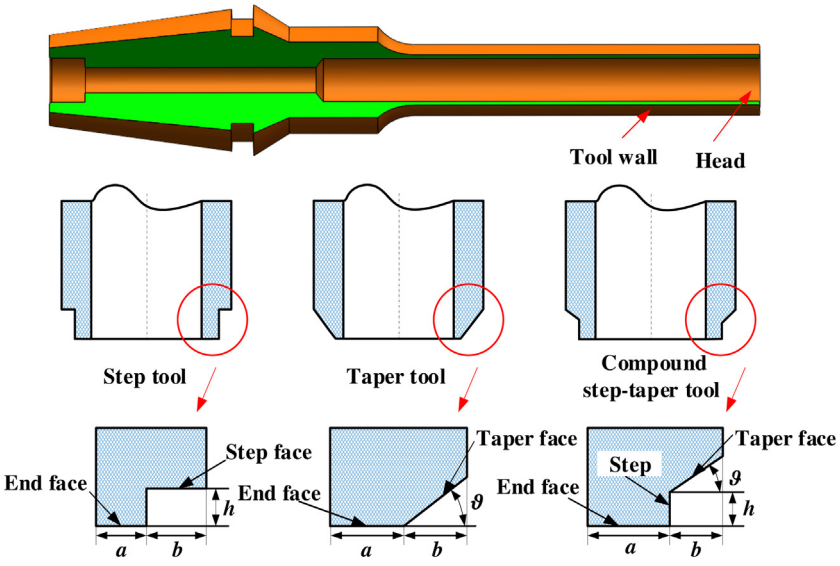

Fig. 3. Inheritance of step-taper comound tool from the step tool and the taper tool.

cutting force (F_c) can be calculated using the following system of equations [18,29]:

$$\begin{cases} d_t = kp^{\alpha}c_0^{2\alpha} \\ F_c = pc_0 \end{cases} \quad (1)$$

where, k is a scale factor, p is the cutting force density per unit of tool wall thickness, and c_0 is the wall thickness of the tool. α is a dimensionless constant factor that can be obtained from experiment results. From the authors' previous studies, $\alpha \approx 0.67$ [18,29] in RUM of brittle materials.

According to Eq. (1), for a certain cutting force density, which is determined by processing parameters such as spindle speed and feed rate, a certain critical value of d_t always exists for Eq. (1) to be satisfied. The edge chipping at the hole exit is bound to form regardless of the optimized processing parameters.

Before the formation of edge chipping, the following inequality for the undrilled thickness (d) and cutting force is satisfied:

$$d > kp^{\alpha}c_0^{2\alpha} \quad (2)$$

If Eq. (2) could always be satisfied at the hole exit during drilling, theoretically, edge chipping would not occur. This is interpreted to mean that the cutting force (pc_0) can gradually decrease when the undrilled thickness (d) decreases at the hole exit. One method is to control the cutting force density (p) by changing parameters such as reducing the feed rate. This method has a limitation; specifically, when the feed rate is quite low, a creep phenomenon of the machine tools aggravates the edge chipping defect because of the abrupt impact of the tool on the workpiece material [31]. The other method is to decrease c_0 via tool design. Fig. 2(c) and (d) present two ways to construct a wedge-type contact structure between the tool end face and the workpiece. Both ways can decrease c_0 at the hole exit.

In Fig. 2(c), the workpiece outlined is the wedge-type, which can be achieved using the step tool (as presented in Fig. 3(a)). In Fig. 2(d), the tool end face is the wedge-type, which can be achieved using a taper tool (as presented in Fig. 3(b)). It has been reported in the authors' previous studies [29,31] that both the step tool and taper tool demonstrate effective performance in terms of reducing edge chipping, although both new types of tools have corresponding limitations. The compound step-taper tool is presented in Fig. 3(c). It is composed of a compound type of the step tool and taper tool. Actually, the step tool or taper tool is a specific mode of the compound tool. As presented in Fig. 3, when $\vartheta = 0$, the compound tool degrades into the step tool. On the other hand, when $h = 0$, the compound tool degrades into the taper tool.

Table 1
Material properties.

Property	Unit	Quartz glass
Young's modulus	GPa	76.7
Vickers hardness	GPa	9.5
Fracture toughness	MPa·m$^{1/2}$	0.71
Density	g/cm^3	2.2
Poisson ration	/	0.17

3. Experiment design

The RUM machine used in this study was an Ultrasonic 50, produced by the DMG Company in Germany. The ultrasonic spindle is the key component of the RUM machine. The corresponding maximum allowable spindle speed under the ultrasonic mode was 6000 rpm. The ultrasonic spindle comprised an ultrasonic power supply, a transducer, an amplitude transformer, and a diamond core tool. A 50 Hz AC electrical current was converted by the ultrasonic power supply to an ultrasonic frequency (approximately 20 kHz) output. The frequency of the ultrasonic power supply could be adjusted freely from 16.5 kHz to 30 kHz, enabling the researcher to tune the ultrasonic spindle to satisfy different natural frequencies of tools. Then, the piezoelectric transducer converted the ultrasonic frequency AC current into mechanical vibration. The amplitude transformer and diamond core tool were designed to amplify the mechanical vibration of the transducer in a usable value that was efficient for material removal during RUM.

As illustrated in Fig. 4, two clamps mounted on a fixture were used to hold the workpiece. A hole of 20 mm in diameter and 12 mm in depth was in the middle face of the fixture to prevent tool knocking on the machined cylinder. The workpiece samples used were 30 mm × 30 mm × 8 mm quartz glass. Material properties of the quartz glass are listed in Table 1. Two different types of diamond core tools (a common tool and the compound step-taper tool) were used to drill the workpiece. The dimensions of the corresponding tool heads are demonstrated in Fig. 4(b) and (c). Both tools were electroplated with diamond abrasives with a grit size of D107.

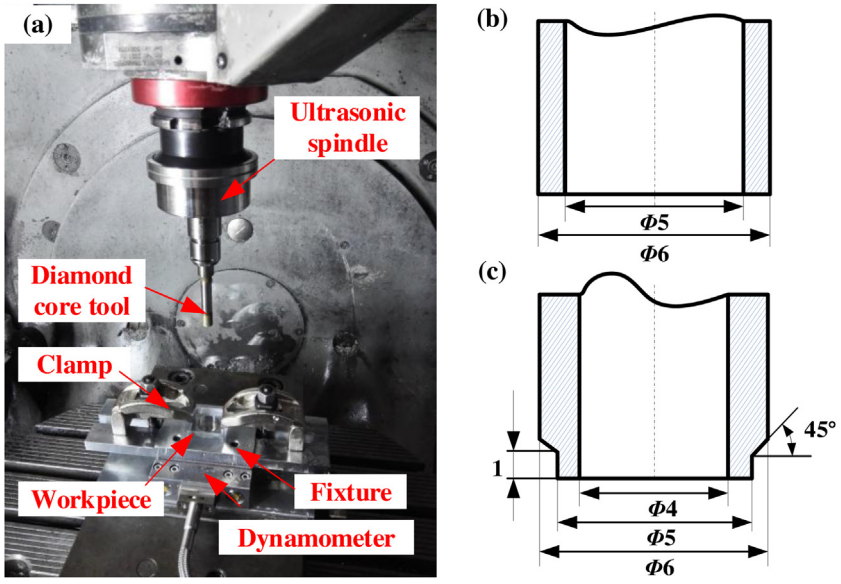

Fig. 4. Experiment setup.

Table 2
Process parameters.

Tool type	Spindle speed (rpm)	Feedrate (mm/min)
Common tool	3000, 4000	2, 3, 4
Compound tool	3000, 4000	2, 3, 4

Several drilling tests were performed to evaluate the feasibility of using the compound step-taper tool to reduce edge chipping at the hole exit. The processing parameters (feed rate and spindle speed) are listed in Table 2. Each experiment was repeated twice to reduce random error. The Ultrasonic 50 was tuned at the corresponding resonant frequency, where the ultrasonic amplitude reached the corresponding peak. Because the resonant frequency of the RUM machine was relative to the specific tool that was mounted, the tuning frequency of the Ultrasonic 50 when two tools were mounted was different. A laser fiber vibrometer (LK-H008, KEYENCE, Japan) was used to measure the resonant frequency and ultrasonic amplitudes. The ultrasonic amplitude could be calculated from the sine motion curve obtained using the laser fiber vibrometer when the sampling frequency was set at 392 kHz and the resolution ratio was set at 0.1 mm. The resonant frequency values of the Ultrasonic 50 when the common tool and compound tool were mounted were 18.45 kHz and 18.10 kHz respectively. The ultrasonic amplitudes of both tools when the Ultrasonic 50 was adjusted at the corresponding resonant frequencies were 7–8 μm. Ideally, drilling tests should be performed at the same ultrasonic parameters. Fortunately, differences in ultrasonic parameters between the two tools were sufficiently low and could be neglected for the experimental requirements. Considering the unavoidable effects of the cutting force on the ultrasonic amplitude stability, the ultrasonic power was monitored during drilling to guarantee that the RUM machine worked well. Both inner and outer recycled coolants were used during drilling tests.

As presented in Fig. 4, a dynamometer (Kistler 9256C2, Switzerland) was used to measure the cutting forces during drilling. A charge amplifier (5070A) amplified the cutting forces signal from the dynamometer. Then, a data acquisition card recorded the cutting force signals. The recorded data were then saved and processed using the commercial software Dynoware, which was provided by Kistler Co., Ltd. The resonant frequency of the dynamometer (Kistler 9256C2) was quite low (4.6 kHz) compared to the ultrasonic vibration frequency. Therefore, it was impossible to acquire the force variation within a vibration cycle. The sampling frequency increase was meaningless in this situation. Thus, the measurement sampling frequency was set at only 100 Hz.

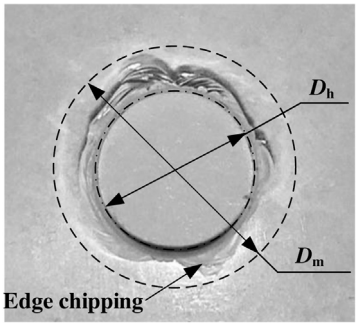

Fig. 5. Definition of edge chipping size.

The edge chipping size is usually used as a criterion to evaluate the hole exit quality [18]. Two parameters that can define the degree of edge chipping are the edge chipping width (d_s) and edge chipping thickness (d_t). Because d_s increases monotonically with d_t [23], only d_s was used for the edge chipping size in this study. As presented in Fig. 5, the edge chip width (d_s) can be defined using the following equation:

$$d_s = \frac{D_m - D_h}{2} \tag{3}$$

where D_m is the maximum diameter of the edge chipping profile and D_h is the hole diameter. An optical microscope (55XA; Shanghai Optical Instrument Factory No. 6, Shanghai, China) was used to measure the edge chipping size at the hole exit.

4. Results and discussion

4.1. Effectiveness of compound tool on edge chipping reduction

Table 3 presents typical images of edge chipping at the hole exit that were obtained using different types of tools. The corresponding processing conditions were a spindle speed of 3000 rpm and feed rate of 3 mm/min. As presented in Table 3, the hole exit quality when using the compound tool was significantly better than that

Table 3
Images of edge chipping at hole exit.

Tool type	Compound tool	Common tool
Edge chipping		

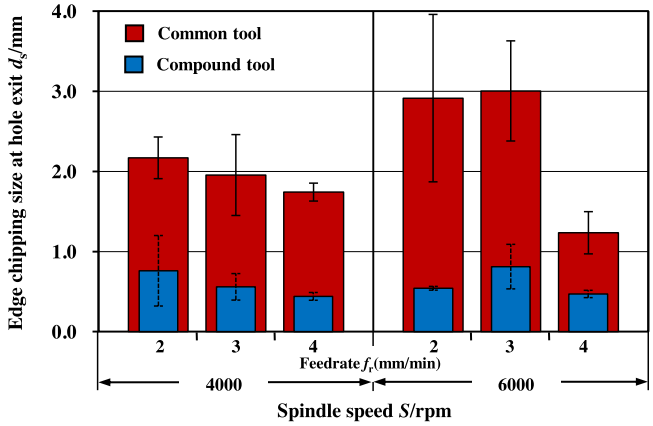

Fig. 6. Comparison of edge chipping at hole exit with different tools.

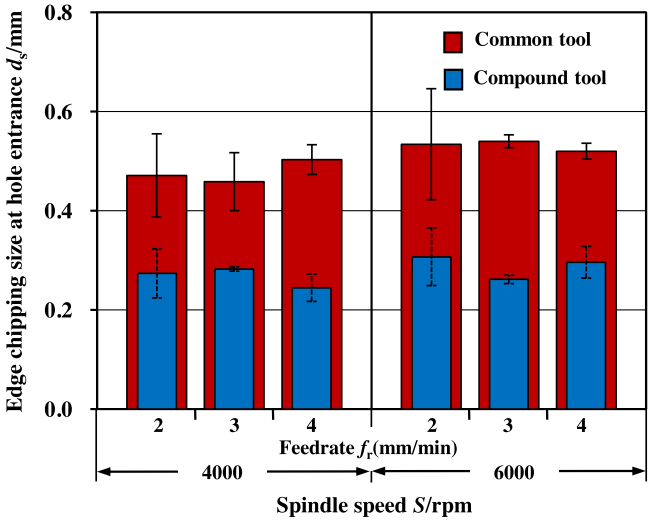

Fig. 7. Comparison of edge chipping at hole entrance with different tools.

when using the common tool. Fig. 6 presents a quantitative comparison of edge chipping defects when different types of tools were used. The error bars for a certain processing condition included the upper deviation (e_{upper}) and lower deviation (e_{lower}). As illustrated in the experimental design, each experiment under a certain processing condition was repeated twice. Thus, two sets of data for edge chipping size were obtained under a certain processing condition. The upper deviation (e_{upper}) was calculated using the maximum value of two edge chipping sizes minus the average value of two edge chipping sizes. The lower deviation (e_{lower}) was calculated using the average value of two edge chipping sizes minus the minimum value of two edge chipping sizes.

As presented in Fig. 6, using the compound tool significantly reduced the edge chipping size in comparison with that when the common tool was used. From calculations, the reduction rates of the edge chipping size at the hole exit were as high as 60%. Also, it was derived from the error bars in Fig. 6 that using the compound tool improved the stability of the hole exit quality. Because of the low toughness of brittle materials, material strength is highly dependent on crack size. The formation of edge chipping at the hole exit during RUM of a brittle material is a typical brittle fracture phenomenon. Both the cutting force and machining induced cracks affect the formation of edge chipping. By contrast, the distribution and magnitude of machining-induced cracks are complicated and stochastic to a certain extent [32,33]. This was the reason for the usual high distribution width of the edge chipping size even under identical processing conditions. Moreover, as presented in Fig. 6, the distribution width of the edge chipping size obtained when the compound tool was used was significantly lower than the edge chipping size when the common tool was used. When the common tool was used, the maximum distribution width of the edge chipping size reached 2 mm. In contrast, when the compound tool was used, the maximum distribution width of the edge chipping size was less than 1 mm.

According to the results presented in Fig. 6, with the compound tool, the error bars at a spindle speed of 6000 rpm and a feed rate of 2 mm/min were significantly smaller than the error bars at a spindle speed of 4000 rpm of spindle speed and a feed rate of 2 mm/min. However, a significantly stable machining performance at a spindle speed of 6000 rpm could not be concluded. This was because when the feed rate was 3 mm/min, the error bars for a spindle speed of 6000 rpm were even higher than the error bars for a spindle speed of 4000 rpm. The effects of processing parameters including the spindle speed and feed rate on the stability of machining performance could not be summarized as a general rule. Furthermore, because performance evaluation of the compound tool was the focus of this research, the irregular effects of processing parameters would not be against the conclusion that the compound tool could have a significantly more stable machining performance than the common tool.

On the other hand, the edge chipping size at the hole exit was expected to increase with a spindle speed decrease or feed rate increase [18,25,30]. As presented in Fig. 6, variations in the edge chipping size at the hole exit did not follow the aforementioned classic conclusion [18,25,30]. This inconsistency was also because of the probabilistic nature of the edge chipping formation. Only when there were a high number of examined parameters and sufficient width, did the expected variation tendency of the edge chipping size at the hole exit have certain abnormalities [31]. The abnormalities involved in the data (Fig. 6) demonstrated the low reliability of the improved hole exit quality via the feed rate reduction or spindle speed increase. In contrast with the processing parameter optimization, using the compound tool to reduce the edge chipping size at the hole exit proved significantly reliable.

Therefore, the experimental results (Fig. 6) indicated that using the compound tool could improve the hole exit quality, not only through reducing the edge chipping size, but also through improving the corresponding stability. Also, reducing the edge chipping size at the hole exit using the compound tool was more reliable than the corresponding reduction obtained via optimization of the processing parameters.

Previously, edge chipping at the hole exit was considered to be the major weakness that restricted improvement of hole-manufacturing quality. The compound tool application changed this situation. To further improve the entire quality of the hole, it was necessary to address the edge chipping defect at the hole entrance. Fig. 7 presents the edge chipping size results at the hole entrance. As illustrated in Fig. 7, using the compound tool reduced the edge chipping size at the hole entrance by 35%–50% compared with the size obtained using the common tool. It can also be observed by comparing Figs. 6 and 7 that edge chipping at the

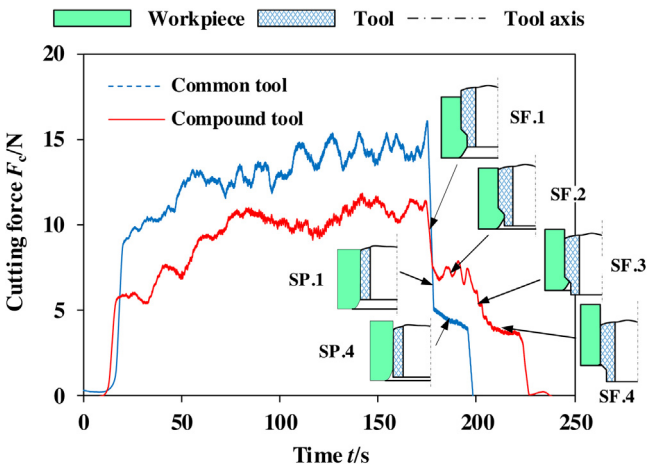

Fig. 8. Cutting force variations at hole exit.

hole exit when the compound tool was used was similar in size (approximately of 0.5 mm) to chipping at the hole entrance when the common tool was used. It is well known that the edge chipping size at the hole entrance is usually significantly smaller than that at the hole exit. Using the compound tool, the minimum edge chipping size at the hole exit could be smaller than 0.35 mm, which is the same magnitude as the edge chipping size at the hole entrance. Actually, it became difficult to identify the hole entrance or exit simply by observing the edge chipping when the compound tool was used.

4.2. Mechanism of edge chipping reduction when using the compound tool

Because the cutting force is the driving factor that results in the formation of edge chipping at the hole exit, the cutting force variations contain the information regarding the formation mechanism of edge chipping at the hole exit. Fig. 8 presents typical cutting force curves of using both the common tool and compound tool with a spindle speed of 3000 rpm and feed rate of 3 mm/min. As seen in Fig. 8, edge chipping occurred almost simultaneously when the different tools were used, indicating that the edge chipping occurred with the same undrilled thickness. This experimental result was consistent with the predictive result of Eq. (1). As illustrated in Fig. 4, the end face wall thickness of the compound tool was identical to the common tool. According to Eq. (1), the undrilled thickness when edge chipping occurs should be identical between different tools with the same wall thickness of the end face. In addition, as seen in Fig. 8, the actual earlier occurrence of edge chipping with the common tool should be attributed to the corresponding slightly higher diameter of the end face.

As seen in Fig. 8, an apparent difference in cutting force variation at the hole exit using different tools was identified. In Fig. 8, the cutting forces at the hole exit were divided into several sub-states for detailed exploration. Specifically, the cutting force at the hole exit using the compound tool was divided into four sub-states: SF.1, SF.2, SF.3, and SF.4. The cutting force at the hole exit using the common tool was divided into two sub states: SP.1 and SP.4.

At the SF.1 or SP.1 states, the cutting force decreased abruptly due to the formation of edge chipping that was induced by the end face of the compound tool or the common tool. At the SF4 and SP.4 states, the diamond abrasives of the tool end face or the taper face finished the machining, whereas the diamond abrasives of the tool wall face still continued to finish the hole wall surface. With an improvement in the hole surface quality, the cutting force decreased quite slowly. The presence of the SF.2 and SF.3 states was the unique feature of the cutting force when the compound tool was used compared to that when the common tool was used. At the SF.2 state, the taper face continued to machine the material, resulting in a relatively unapparent change in the average value of the cutting force. At the SF.3 state, the contact area between the tool's taper face and the workpiece material decreased as the drilling depth increased. This led to a gradual decrease of the cutting force. Though the undrilled thickness (d) of the material decreased as the drilling depth increased at the hole exit, the cutting force also decreased, leading to suppression of new edge chipping formation. Simultaneously, the taper face of the compound tool removed the old edge chipping that was induced by the tool end face.

According to the research results reported by Lv et al. [34], the formation mechanism of edge chipping at the hole entrance was rather different from the formation mechanism of edge chipping at the hole exit. The formation of edge chipping at the hole exit is a macroscopic fracture phenomenon under the integrated cutting force of all of the abrasives that take part in the machining. In contrast, formation of edge chipping at the hole entrance is a microscopic fracture phenomenon that directly results from the material removal by each individual abrasive [18]. Quite different morphologies of edge chipping at the hole exit and entrance verified the aforementioned differences in the corresponding formation mechanisms. The edge chipping defect at the hole exit was continuous; however, the edge chipping defect at the hole entrance was serrated. Therefore, the edge chipping reduction mechanism at the hole entrance when the compound tool was used should be attributed to the material removal mechanism.

Because of ultrasonic vibration of the tool, diamond abrasives do not always contact the workpiece material. In each vibration cycle, diamond abrasive penetrates the workpiece to a certain depth for a certain period. As illustrated in Fig. 9(a), material removal during the RUM of brittle materials is an indentation fracture process. Penetration can be divided into two sub processes: loading and unloading. In the loading process, the moving direction of the diamond abrasive is toward the workpiece. During the loading process, plastic deformation zones and radial cracks are produced [35]. Radial cracks remain beneath the workpiece surface as subsurface damage. In the unloading process, the moving direction of the diamond abrasive is away from the workpiece. During the unloading process, lateral cracks form because of the residual stress induced by plastic deformation. The lateral cracks propagate and interact with each other, leading to material removal. When lateral cracks are produced by the outermost abrasives of the tool end face or the taper face, the lateral cracks propagate toward the workpiece surface, and edge chipping at the hole entrance occurs [34].

As shown in Fig. 9(b), when the common tool was used, the diamond abrasives of the tool end face concurrently took part in material removal at the hole entrance. When this occurred, the outermost diamond abrasives dominated the formation of edge chipping defects at the hole entrance. In contrast, when the compound tool was used, the diamond abrasives of the tool's taper face successively took part in the material removal. As shown in Fig. 9(c) and (d), the outermost abrasives of the tool's taper face were the last abrasives that took part in the material removal. In this situation, the residual lateral cracks that were produced by the second outermost abrasives could significantly affect indentation of the outermost abrasives in terms of shielding effects of the cracks. Residual lateral cracks beneath the workpiece surface reduced the equivalent rigidity of the material and consumed the impact energy [36] when the outermost abrasives initiated material removal. On one hand, residual lateral cracks restrained propagation of radial cracks by continually inhibiting the tensile stress that was produced during the loading of the outermost abrasives. On the other hand, as demonstrated in the previous paragraph, plastic deformation during the loading process was essential for the forma-

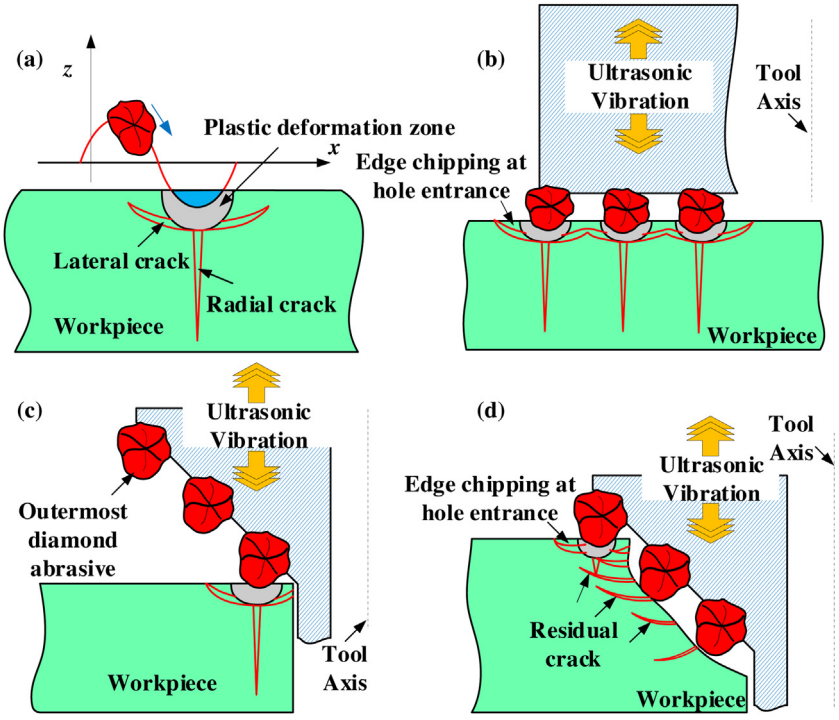

Fig. 9. Illustration of edge chipping formation mechanim at the hole entrance. (a) Material removal model of RUM. (b) Formation of edge chipping at hole entrance using the common tool. (c) and (d) Formation of edge chipping at hole entrance using the compound tool.

tion and propagation of lateral cracks during the unloading process. The residual lateral cracks that were produced by the second outermost abrasives suppressed plastic deformation during the loading process of the outermost abrasives, thus inhibiting formation and propagation of lateral cracks during the unloading process of the outermost abrasives.

The material removal process in RUM is supposed to be an indentation process in the edge chipping formation mechanism analysis at the hole entrance without the cutting velocity consideration. In fact, this kind of material removal model, as proposed by Pei et al. [37], has achieved high success in modeling the processing outputs of RUM, such as cutting force [16,38], subsurface damage depth [39], and edge chipping size [18]. The effects of spindle speed on crack propagation are generally attributed to the corresponding effects on indentation depth and scratching length of the diamond abrasive at the workpiece surface. In addition, according to the results of Lv et al. [34], the cutting velocity indeed affects the propagation length of lateral cracks via the strain rate effect on the material property in contrast with only via the indentation depth change. This might be one reason that accounts for the predictive error of these processing output models that are developed on the basis of the indentation process. Moreover, this would not reduce the mechanism validity of edge chipping reduction at the hole entrance using the compound tool, as illustrated in Fig. 9 because the edge chipping sizes with different tools were compared with identical spindle speeds. Furthermore, it is believed that the shielding effect of residual cracks on the propagation of lateral cracks would still be effective under various spindle speeds.

4.3. Role of step in compound tool effectiveness

Based on the analysis of the previous section, the taper face is the key to observing the compound tool effectiveness on the edge chipping reduction at the hole exit and the entrance. The step of the compound tool is not correlated with the edge chipping formation at the hole entrance. However, in terms of the edge chipping formation at the hole exit, the compound tool step plays an important role. As shown in Fig. 10, to guarantee the compound tool effectiveness on the edge chipping reduction at the hole exit, the initial edge chipping should occur at the outer side of the tool end face, as in Fig. 10(c), rather than at the outer side of the tool's taper face, as in Fig. 10(b).

Based on Eq. (2), the variables presented in Fig. 10(a) satisfied the following inequalities:

$$d + h + b\tan\vartheta \geq kp^{\alpha}(a+b)^{2\alpha} \tag{4}$$

$$d \geq kp^{\alpha}a^{2\alpha} \tag{5}$$

where a, b, h, and ϑ are characteristic parameters of the compound tool. a is the end face thickness, b is the taper face thickness, h is the step height, and ϑ is the characteristic angle of the taper face. When edge chipping occurred at the outer side of the tool's taper face, the equal sign of Eq. (4) was established. When the edge chipping occurred at the outer side of the tool's end face, the equal sign of Eq. (5) was established. The equal signs of Eqs. (4) and (5) were not always simultaneously established. During RUM, when the undrilled thickness decreased, the equal signs of Eqs. (4) and (5) were established successively. When the equal sign of Eq. (4) was established first, using the compound tool did not reduce the edge chipping size at the hole exit. By contrast, when the equal sign of Eq. (5) was established first, using the compound tool was effective for reducing edge chipping at the hole exit.

It can be derived from Eqs. (4) and (5) that the step height (h) and the characteristic angle (ϑ) are critical for guaranteeing that the equal sign of Eq. (5) is established before the equal sign of Eq. (4). The critical values can be derived from the simultaneous establishment of the equal signs of Eqs. (4) and (5):

$$h_c + b\tan\vartheta_c = kp^{\alpha}\left((a+b)^{2\alpha} - a^{2\alpha}\right) \tag{6}$$

where h_c is the critical step height and ϑ_c is the critical characteristic angle.

Eq. (6) demonstrates the role of the step in the compound tool effectiveness. Based on the author's previous investigation, ϑ_c is

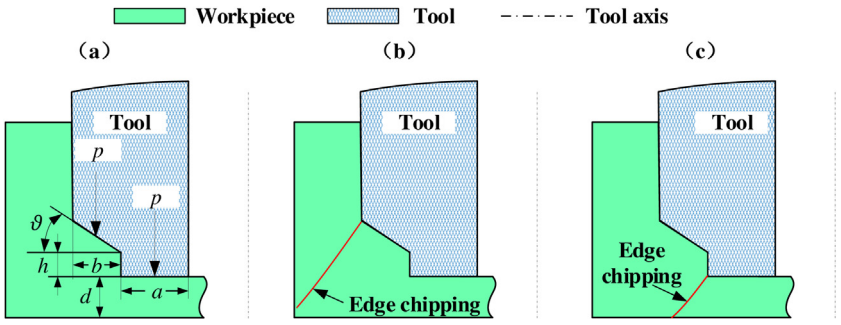

Fig. 10. Edge chipping formation modes using the compound tool: (a) force scheme, (b) edge chipping at the taper face outer side, and (d) edge chipping at the end face outer side.

typical for the taper tool [31]. The characteristic angle (ϑ) should exceed the corresponding critical value (ϑ_c) [31] to guarantee the taper tool effectiveness on reducing edge chipping. Simultaneously, a higher feed rate corresponds to a higher cutting force density and to a higher ϑ_c [31]. According to Eq. (6), the step presence is beneficial in reducing ϑ_c and consequently in extending the effective application range of the compound tool to higher machining efficiency.

In the authors' previous study [29], when the step tool was used without the taper face, the rate of reducing edge chipping at the hole exit can reach approximately 60% compared to the common tool. When step tools with or without a taper face were used, both of the reduction mechanisms of edge chipping at the hole exit were the development of wedge-type contact structures between the tool and the workpiece to gradually reduce the cutting force. By contrast, the specific methods for developing wedge-type contact structures were different when the step tools with or without a taper face were used. When the step tool was used without a taper face, the wedge-type contact structure was established by the step face with the initial edge chipping profile. Moreover, when the step tool was used with a taper face, the wedge-type contact structure could be established by the taper face with the undrilled workpiece even without the initial edge chipping profile. Because of the corresponding persistent enhancement of the aforementioned wedge-type contact structure, when a taper face was used on the step tool, the compound tool had quite reliable exit edge chipping suppression performance when inclined holes were drilled and also improved the entrance edge quality.

5. Conclusions

In this study, a compound step-taper tool for rotary ultrasonic machining (RUM) was used to further reduce the edge chipping phenomenon when holes are drilled in brittle materials. Drilling tests on quartz glass were conducted to evaluate the effectiveness of the compound tool. The mechanism of reducing edge chipping using the compound tool was derived from detailed observation of the cutting force. The experimental results demonstrated that the compound tool contributed significantly to reducing the edge chipping size during RUM of quartz glass.

(1) The compound tool contributed to reducing the edge chipping size at the hole exit by 60%–80% and also contributed to improved stability. Also, the improvement of hole exit quality using the compound tool was significantly reliable compared to that obtained via optimization of the processing parameters. The edge chipping reduction mechanism at the hole exit was a decrease in the cutting force as the undrilled thickness decreased with use of a taper face. Moreover, the tool's taper face eliminated the previous edge chipping that was induced by the tool's end face.

(2) The compound tool can contribute to reducing the edge chipping size at the hole entrance by 35%–50% because of the shielding effect of residual cracks that were produced by the second outermost abrasives of the tool's taper face. The effect suppressed initiation and propagation of lateral cracks that were produced by the outermost abrasives of the tool's taper face.

(3) The compound tool's step face was beneficial for the effectiveness of the compound tool in hole exit quality improvement by reducing the critical characteristic angle of the tool's taper face.

Conflict of interest

The authors declare that they have no conflict of interest.

Acknowledgements

We gratefully acknowledge the financial support for this research from the National Natural Science Foundation of China (Grant no. 51475260) and the National Natural Science Foundation of China (Grant no. 51761145103).

References

[1] Chen JB, Fang QH, Wang CC, Du JK, Liu F. Theoretical study on brittle–ductile transition behavior in elliptical ultrasonic assisted grinding of hard brittle materials. Precis Eng 2016;46:104–17.
[2] Wang Y, Lin B, Wang S, Cao X. Study on the system matching of ultrasonic vibration assisted grinding for hard and brittle materials processing. Int J Mach Tools Manuf 2014;77:66–73.
[3] Guo J, Chen J, Li J, Fang Q, Liu Y. Study on subsurface-inclined crack propagation during machining of brittle crystal materials. Appl Phys A 2016;122:493.
[4] Zhang X, Arif M, Liu K, Kumar AS, Rahman M. A model to predict the critical undeformed chip thickness in vibration-assisted machining of brittle materials. Int J Mach Tools Manuf 2013;69:57–66.
[5] Wang C, Chen J, Fang Q, Liu F, Liu Y. Study on brittle material removal in the grinding process utilizing theoretical analysis and numerical simulation. Int J Adv Manuf Technol 2016;87:2603–14.
[6] Li G, Yu Z, Song J, Li C, Li J, Natsu W. Material removal modes of quartz crystals by micro usm. Procedia CIRP 2016;42:842–6.
[7] Zheng K, Li Z, Liao W, Xiao X. Friction and wear performance on ultrasonic vibration assisted grinding dental zirconia ceramics against natural tooth. J Braz Soc Mech Sci Eng 2017;39(3):833–43.
[8] Zhou M, Zheng W. A model for grinding forces prediction in ultrasonic vibration assisted grinding of sicp/al composites. Int J Adv Manuf Technol 2016;87:3211–24.
[9] Tesfay HD, Xu Z, Li ZC. Ultrasonic vibration assisted grinding of bio-ceramic materials: an experimental study on edge chippings with hertzian indentation tests. Int J Adv Manuf Technol 2016;86:3483–94.
[10] Li W, Zhang R, Liu Y, Wang C, Wang J, Yang X, et al. Effect of different parameters on machining of sic/sic composites via pico-second laser. Appl Surf Sci 2016;364:378–87.
[11] Liu Y, Wang C, Li W, Yang X, Zhang Q, Cheng L, et al. Effect of energy density on the machining character of c/sic composites by picosecond laser. Appl Phys A 2014;116:1221–8.
[12] Samant AN, Dahotre NB. Laser machining of structural ceramics-a review. J Eur Ceram Soc 2009;29:969–93.

[13] Wei C, Zhao L, Hu D, Ni J. Electrical discharge machining of ceramic matrix composites with ceramic fiber reinforcements. Int J Adv Manuf Technol 2013;64:187–94.
[14] Singh RP, Singhal S. Rotary ultrasonic machining: a review. Mater Manuf Process 2016;31:1795–824.
[15] Lv D. Influences of high-frequency vibration on tool wear in rotary ultrasonic machining of glass bk7. Int J Adv Manuf Technol 2015;84:1443–55.
[16] Cong WL, Pei ZJ, Sun X, Zhang CL. Rotary ultrasonic machining of cfrp: a mechanistic predictive model for cutting force. Ultrasonics 2014;54:663–75.
[17] Mizobuchi Akira, Honda Kota, Ishida Tohru. Improved chip discharge in drilling of glass plate using back tapered electroplated diamond tool. Int J Precis Eng Manuf 2017;18(9):1197–204.
[18] Wang J, Feng P, Zhang J, Zhang C, Pei Z. Modeling the dependency of edge chipping size on the material properties and cutting force for rotary ultrasonic drilling of brittle materials. Int J Mach Tools Manuf 2016;101:18–27.
[19] Feng P, Wang J, Zhang J, Zheng J. Drilling induced tearing defects in rotary ultrasonic machining of c/sic composites. Ceram Int 2017;43:791–9.
[20] Ding K, Fu Y, Su H, Chen Y, Yu X, Ding G. Experimental studies on drilling tool load and machining quality of c/sic composites in rotary ultrasonic machining. J Mater Process Tech 2014;214:2900–7.
[21] Jain AK, Pandey PM. Modeling of un-deformed chip thickness in rum process and study of size effects in μ-rum. Ultrasonics 2017;77:1–16.
[22] Li ZC, Cai L, Pei ZJ, Treadwell C. Edge-chipping reduction in rotary ultrasonic machining of ceramics: finite element analysis and experimental verification. Int J Mach Tools Manuf 2006;46:1469–77.
[23] Wang J, Zha H, Feng P, Zhang J. On the mechanism of edge chipping reduction in rotary ultrasonic drilling: a novel experimental method. Precis Eng 2016;44:231–5.
[24] Cong WL, Feng Q, Pei ZJ, Deines TW, Treadwell C. Edge chipping in rotary ultrasonic machining of silicon. Int J Manuf Res 2012;7:311–29.
[25] Jiao Y, Liu WJ, Pei ZJ, Xin XJ, Treadwell C. Study on edge chipping in rotary ultrasonic machining of ceramics: an integration of designed experiments and finite element method analysis. J Manuf Sci Eng 2005;127:752–8.
[26] Liu JW, Baek DK, Ko TJ. Chipping minimization in drilling ceramic materials with rotary ultrasonic machining. Int J Adv Manuf Technol 2014;72:1527–35.
[27] Gong H, Fang FZ, Zhang XF, Du J, Hu XT. Study on the reduction strategy of machining-induced edge chipping based on finite element analysis of in-process workpiece structure. J Manuf Sci Eng ASME 2013;135:11017.
[28] Chen Y, Pei ZJ, Treadwell C. Investigations on edge chipping in rotary ultrasonic machining using finite element analysis. Mater Sci Forum 2006;532:969–72.
[29] Wang J, Feng P, Zhang J. Reduction of edge chipping in rotary ultrasonic machining by using step drill: a feasibility study. Int J Adv Manuf Technol 2016;87:2809–19.
[30] Qin N, Pei ZJ, Cong WL, Guo DM. Effects of tool design on edge chipping in ultrasonic-vibration-assisted grinding. In: ASME 2010 international manufacturing science and engineering conference; 2010. p. 147–54.
[31] Wang J, Feng P, Zhang J. Investigations on the edge-chipping reduction in rotary ultrasonic machining using a conical drill. Proc Inst Mech Eng Part B J Eng Manuf 2016;230(7):1254–63.
[32] Lv D, Tang Y, Wang H, Huang Y. Experimental investigations on subsurface damage in rotary ultrasonic machining of glass bk7. Mach Sci Technol 2013;17:443–63.
[33] Lv D, Huang Y, Tang Y, Wang H. Relationship between subsurface damage and surface roughness of glass bk7 in rotary ultrasonic machining and conventional grinding processes. Int J Adv Manuf Technol 2013;67:613–22.
[34] Lv D, Zhang Y, Peng Y. High-frequency vibration effects on hole entrance chipping in rotary ultrasonic drilling of bk7 glass. Ultrasonics 2016;72:47–56.
[35] Cong W, Pei Z. Process of ultrasonic machining. In: Nee AYC, editor. Handbook of manufacturing engineering and technology. London: Springer; 2014. p. 1629–50.
[36] Lv D, Huang Y, Wang H, Tang Y, Wu X. Improvement effects of vibration on cutting force in rotary ultrasonic machining of bk7 glass. J Mater Process Technol 2013;213:1548–57.
[37] Pei ZJ, Prabhakar D, Ferreira PM, Haselkorn M. A mechanistic approach to the prediction of material removal rates in rotary ultrasonic machining. J Eng Ind 1995;117:142–51.
[38] Liu D, Cong WL, Pei ZJ, Tang Y. A cutting force model for rotary ultrasonic machining of brittle materials. Int J Mach Tools Manuf 2012;52:77–84.
[39] Wang J, Zhang C, Feng P, Zhang J. A model for prediction of subsurface damage in rotary ultrasonic face milling of optical k9 glass. Int J Adv Manuf Technol 2016;83:347–55.